Mon. Not. R. Astron. Soc. **000**, 1–12 (2010) Printed 26 July 2011 (MN LATEX style file v2.2)

Occurrence of the 2:1 commensurability in a gas giant – Super-Earth system

E. Podlewska-Gaca⋆ and E. Szuszkiewicz†
Institute of Physics and CASA, University of Szczecin, ul. Wielkopolska 15, 70-451 Szczecin, Poland*

Accepted; Received; in original form

ABSTRACT

We investigate how the conditions occurring in a protoplanetary disc may determine the final structure of a planetary system emerging from such a disc. We concentrate our attention on the dynamical interactions between disc and planets leading to orbital migration, which in turn, in favourable circumstances, can drive planets into a mean-motion commensurability. We find that for a system containing a gas giant on the external orbit and a Super-Earth on the internal one, both embedded in a gaseous disc, the 2:1 resonance is a very likely configuration, so one can expect it as an outcome of the early phases of the planetary system formation. Our conclusion is based on an extensive computational survey in which we ask what are the disc properties (the surface density and the viscosity) for which the 2:1 commensurability may be attained. To answer this question we employ a full two-dimensional hydrodynamic treatment of the disc-planet interactions. In general terms, we can claim that the conditions which favour the 2:1 mean-motion resonance exist in the protoplanetary discs with mass accretion rates in the range of $5{\cdot}10^{-9} - 5\cdot10^{-8}$ $M_\odot$/year. For accretion rates higher than those needed for the 2:1 commensurability we observe a variety of behaviours, among them the passage to the 3:2 resonance, the scattering of the Super-Earth or the divergent migration caused by the outward migration of the gas giant. The results we have obtained from numerical simulations are compared with the predictions coming from the existing analytical expressions of the migration speed and the strength of the mean motion resonances. The conditions that we have found for the attainment of the 2:1 commensurability are discussed in the framework of the properties of protoplanetary discs that are known from the observations.

Key words: methods: numerical - planets and satellites: formation

1 INTRODUCTION

Mean-motion resonances are ubiquitous phenomena in planetary systems. They carry important information about the formation processes and the further evolution of those systems. Moreover, their occurrence may increase the chance of detecting planets which happen to be in a resonant configuration (Agol et al. 2005; Holman & Murray 2005). They might also be able to tell us more about the properties of the protoplanetary discs in which planets are born. The increasing number of low-mass planets being discovered in multiple planetary systems (e.g. Mayor et al. 2009a (HD 40307); Mayor et al. 2009b (GJ 581); Lovis et al. 2011 (HD 10180)) is the first strong observational motivation for the studies of planetary formation and evolution. Another motivation is connected with the growing amount of data coming from high angular resolution observations of protoplanetary discs (e.g. Andrews et al. 2009; Hughes et al. 2009; Isella et al. 2010; Olofsson et al. 2011; Huélamo et al. 2011). The excitement in this area of research is stimulated also by the fast progress in theoretical investigations of the orbital migration due to the action of tidal torques (Lin & Papaloizou 1993; Ward 1997; Tanaka et al. 2002; Paardekooper & Papaloizou 2008, 2009). The convergent migration of planets or protoplanetary cores is one of the most promising processes to explain the formation of resonant configurations. Extensive studies of possible resonant structures have been performed among others by Nelson & Papaloizou (2002) and Papaloizou & Szuszkiewicz (2005, 2010). In Nelson & Papaloizou (2002) the possible commensurabilities to be expected in the system of planets in the Jovian mass range are investigated, while in Papaloizou & Szuszkiewicz (2005, 2010) migrating planets in the terrestrial mass range are considered and the conditions for the occurrence of first order mean-motion resonances are provided. Fogg & Nelson

⋆ E-mail: edytap@univ.szczecin.pl (EP)
† E-mail: szusz@fermi.fiz.univ.szczecin.pl (ES)

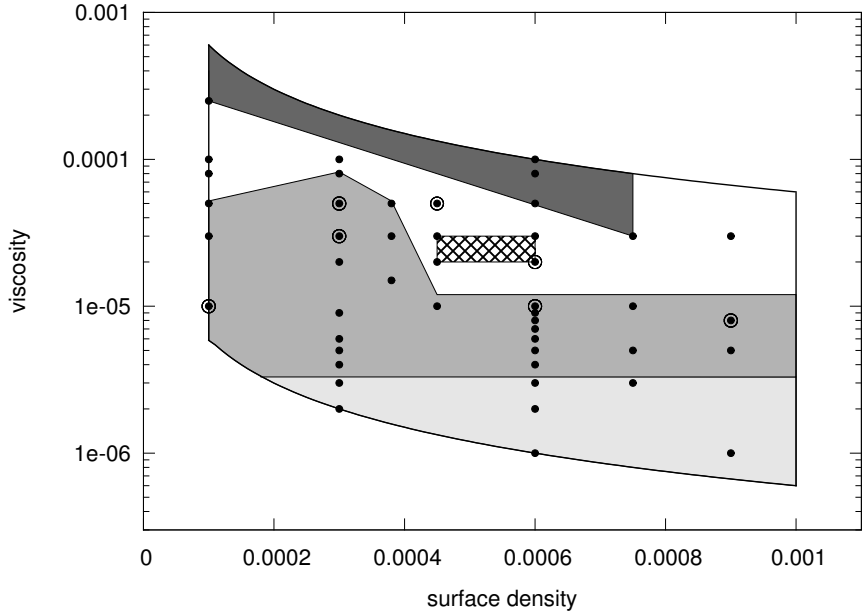

Figure 1. The parameter space of the properties of the protoplanetary discs: surface density - viscosity plane. The central medium gray part denotes the region where planets attain the 2:1 commensurability and the small hatched area favours the formation of the 3:2 resonance. Upper dark gray and lower light gray colours show the parameters for which the migration is divergent, and the white colour denotes the transition region where the variety of behaviours have been observed.

(2007), Zhou et al. (2005), Raymond et al. (2006), Mandell et al. (2007) have shown that terrestrial planets can grow and be retained in the hot-Jupiter systems and that their resonant captures by a gas giant are quite common. In the present paper we consider a system containing a Jupiter-like planet evolving together with a Super-Earth in a gaseous disc. We perform a survey of the different disc properties in which this system is embedded using full hydrodynamical calculations to simulate the dynamical interactions between discs and planets. Our purpose here is to find out what are the conditions for the occurrence of the 2:1 commensurability in such systems and at the same time to get an insight into the environment suitable for the formation of planets on the basis of the existence of certain mean-motion commensurabilities in young planetary systems. It has been shown in Podlewska & Szuszkiewicz (2008, 2009) that in the gas giant – Super-Earth systems the planets embedded in a gaseous disc are easily locked in the commensurabilities if and only if the Super-Earth is located inside the orbit of the gas giant. For this reason, we consider here exactly that kind of configurations in which the Super-Earth is the inner and the gas giant is the outer planet of the system. In the previous paper (Podlewska & Szuszkiewicz 2008), where the same system has been studied, the 2:1 commensurability was not included because of computational limitations.

This paper is organized as follows: In Section 2 we describe how our computational survey has been performed. Next, we illustrate the relevant features of the evolution of Jupiter-like planets in discs with different viscosities. In Section 4 we give the results of our survey presenting different configurations achieved during the tidal evolution of the planets in the disc. These results are compared in Section 5 with the theoretical expectation based on the analytical and semi-analytical expressions for the migration speed of the planets and the strength of the mean motion resonances. In Section 6 we point those observed protoplanetary discs in which the physical conditions that favour the occurrence of the 2:1 resonance are present. Finally, our findings are summarized and discussed in Section 7.

2 SETTING THE SCENE FOR THE SURVEY

In order to determine possible resonances induced by planet migration in the presence of a gaseous disc in a system containing a Super-Earth and a gas giant, we have performed a computational survey by means of full two-dimensional hydrodynamic simulations. The mass of the Super-Earth is taken to be 5.5 $M_\oplus$ and that of the gas giant 1 M_J (here $M_\oplus$ and M_J denote the masses of the Earth and the Jupiter respectively). This pair of planets is used in our simulations as a probe of the disc properties which favour the resonant capture of the Super-Earth by the gas giant. We have fixed the disc aspect ratio to $h = 0.05$, which is a typical value for protoplanetary discs. Herewith, we have assumed for the initial surface density the classical power law parameterization

$$\Sigma(r) = \Sigma_0 \left(\frac{r}{5.2AU}\right)^{-p} \quad (1)$$

with $p = 0$. We will comment on these assumptions in Sections 5 and 6. In our survey different discs will be analyzed, whose properties will be distinguished by using two parameters, namely the surface density value Σ and the coefficient of kinematic viscosity ν, which is constant in space and time. In the following, these two parameters will be referred to as "disc properties". The parameter space for our studies is illustrated in Fig. 1. The value of the surface density Σ varies from 10^{-4} to 10^{-3} in the dimensionless units used in the

code. The unit of mass is the mass of the central star M (here we take $M = M_\odot$) and the unit of length r_p is the initial position of the inner planet (the Super-Earth in our case). The unit of time in the code is given by $(GM/r_p^3)^{1/2}$ (G is the gravitational constant). This quantity amounts to $(1/2\pi)$ times the orbital period of the initial orbit of the Super-Earth. The value of $6 \cdot 10^{-4}$ of the surface density in these units is consistent with the Minimum Mass Solar Nebula (MMSN) (Hayashi 1981) at the present position of Jupiter in our planetary system, i.e. 5.2 AU. The range of the surface densities considered here expressed in physical units is the following: 30 - 300 g/cm^2. In order to constrain the values of the kinematic viscosity ν for our studies, we have used the relation between the kinematic viscosity and the accretion rate $\dot{M}$ observed in T Tauri stars, which are the best laboratories for studying the early stages of planetary evolution. For a stationary thin accretion disc this relation reads

$$\Sigma\nu = \frac{\dot{M}}{3\pi}. \qquad (2)$$

The upper and lower curves in Fig. 1 are the constant accretion rate levels. For the upper curve we have adopted $3 \cdot 10^{-7}$ $M_\odot$/year and for the lower one $3 \cdot 10^{-9}$ $M_\odot$/year, which are typical accretion rates observed in T Tauri stars. The viscosities obtained in this way vary from $6 \cdot 10^{-4}$ to $6 \cdot 10^{-7}$ in terms of the inverse of the Reynolds number at the initial location of the Super-Earth. Those two curves, together with the minimal and maximal values of the surface density, form the region of parameter space which is of interest for our studies. In the region defined in this way we have chosen 47 initial disc configurations for which we have performed numerical simulations. Each black dot in Fig. 1 represents a protoplanetary disc of given surface density and viscosity. The circles around some of the black dots indicate those discs which are of particular interest and are described in detail in the next Sections. The sampling of the parameter space is not uniform. We have calculated the evolution of planets only for those discs which were relevant for our purpose, namely for determining the variety of the final architectures of the planets.

We have performed full two-dimensional hydrodynamic calculations using the grid based code NIRVANA. For details on the numerical scheme and the adopted code see Nelson et al. (2000). The planets interact with each other and with the protoplanetary disc in which they are embedded. These dynamical interactions take place in the central potential of a solar mass host star. The disc is locally isothermal. It extends from 0.33 to 4 in dimensionless units. We use the resolution of 384 x 512 grid cells in the radial and the azimuthal directions respectively. The grid spacing in both coordinate directions is uniform. The computational domain is a ring, in which the azimuthal coordinate ϕ takes its values in the interval $[0, 2\pi]$. We choose open boundary conditions in the radial direction and periodic in the azimuthal one. We do not exclude any material from the Hill sphere and we discuss the consequences of this in Section 5. The potential is softened with the parameter $b = 0.8H$, where H is the semi-thickness of the disc at the planet position. The initial eccentricity of both planets is set to zero.

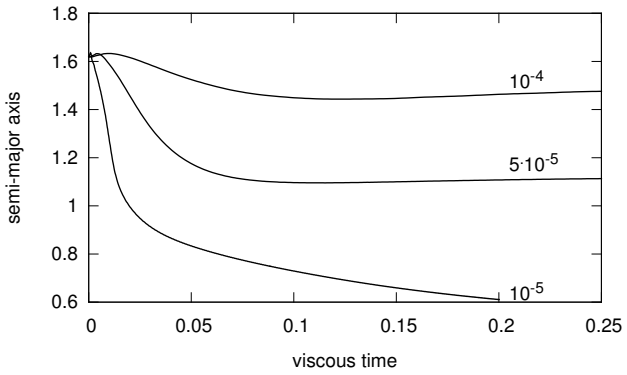

Figure 2. The semi-major axis evolution of the migrating Jupiter-like planet in the disc with different values of the viscosity and with the surface density corresponding to the MMSN at 5.2 AU. The curves are labeled by the value of the viscosity in the disc given in terms of the inverse of the Reynolds number. The 'viscous time' means the time expressed in viscous time units.

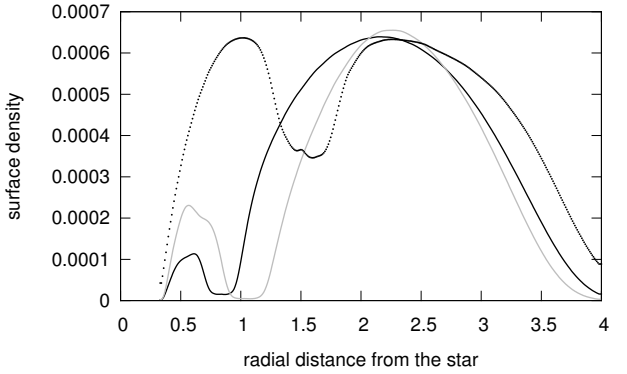

Figure 3. The surface density profiles at 0.05 t_ν for three different viscosities: $5 \cdot 10^{-6}$ (grey line), 10^{-5} (black line) and 10^{-4} (dots).

3 GAS GIANT MIGRATING IN DISCS WITH DIFFERENT VISCOSITIES

It has been established that the migration of the gas giant in protoplanetary discs depends on the value of the viscosity (Lin & Papaloizou 1986, 1993). The viscosity controls the processes responsible for the gap opening in the disc which is crucial for further evolution of the orbit of the planet. We have checked that for viscosities lower than 10^{-5} and typical surface densities, the migration of the Jupiter-like planet in a reasonably good approximation, proceeds on a viscous timescale as in the classical Type II regime.

Relatively recently, Crida & Morbidelli (2007) found that for sufficiently high values of the viscosity, corresponding to Reynolds numbers of around 10^4, the migration of the gas giant tends to change its direction and the planet moves outwards. The values of viscosity for which they have obtained the outward migration of the Jupiter-like planet are present also in our parameter space so, we have been able to verify if the gas giant behaves similarly in the discs analyzed in our survey. The results, illustrated in Fig. 2, show the evolution of the semi-major axis of the Jupiter mass planet placed in the protoplanetary disc with the sur-

face density equal to the MMSN at 5.2 AU and different kinematic viscosities. Following Crida & Morbidelli (2007), in Fig. 2 and in all other figures where time is present, the time is measured in units of the viscous time t_ν, which is defined in the following way

$$t_\nu = \frac{r_p^2}{\nu}. \quad (3)$$

If the viscosity becomes higher than 10^{-5}, the Jupiter migration slows down, and if the viscosity reaches the value of $5 \cdot 10^{-5}$ or higher, the migration of the Jupiter is reversed. It means that the Jupiter-like planet will not be subjected to proper type II migration for sufficiently high disc viscosities. Our results are thus consistent with those obtained by Crida & Morbidelli (2007) despite the differences in the initial surface density profile and the numerical treatment adopted in this paper. To complete the picture of a gas giant migrating in the discs with different viscosities, we present also the surface density profiles (Fig. 3) for three of our simulations characterized by viscosity values of $5 \cdot 10^{-6}$, 10^{-5} and 10^{-4} respectively. All profiles are shown at the same time of the simulations, namely at 0.05 t_ν. This figure clearly illustrates how the gap profile depends on the value of the viscosity. It is also worth mentioning that the mass of the inner disc critically depends on the position of the gas giant with respect to the inner edge of the grid as has been shown by Crida & Morbidelli (2007). The outward migration of the Jupiter has an important consequence for the resonant captures described in Section 4.

4 EXPECTED COMMENSURABILITIES FOR A VARIETY OF PROTOPLANETARY DISC PROPERTIES

The planets have been placed in various discs with surface densities and viscosities taken from the range shown in Fig. 1 and described in Section 2. The initial separation between the planets has been chosen to be slightly larger than that required for the 2:1 resonance. Next, we have followed the evolution of this system for roughly $2 \cdot 10^3$ orbits of the inner planet i.e. the Super-Earth. Depending on the final configuration of the planets, we have divided the whole parameter space into five regions. The medium grey part of the diagram in Fig. 1 is characterized by the fact that the most likely outcome of the evolution of the migrating planets is the resonant capture in the 2:1 commensurability. The disc with properties lying in the small central hatched region favours the formation of the 3:2 resonance. For discs with viscosity smaller than $4 \cdot 10^{-6}$ the differential migration is divergent and we do not expect to find any commensurability in this case. The same is true for discs with surface densities and viscosities taken from the dark grey part of the diagram in Fig. 1. In this region the migration of the Jupiter is directed outward, while the Super-Earth migrates inward, so that the resonant capture is not possible. A transition region in which a variety of different behaviours has been observed is denoted in white.

At this point, we would like to describe briefly the typical behaviour of the system in each region of the parameter space shown in Fig. 1.

4.1 The 2:1 commensurability

The capture in the 2:1 resonance is a very likely outcome of the planet evolution in the disc. Indeed, the medium dark grey region of the diagram in Fig. 1, in which the physical conditions in the disc favour the achievement of just that commensurability, is the most pronounced one. As it turns out from Fig. 1, the best conditions for the occurrence of the 2:1 resonance exist in the region in which the surface densities are relatively low (from 10^{-4} till $3.5 \cdot 10^{-4}$) and the viscosity ranges from $4 \cdot 10^{-6}$ till almost 10^{-4}. For higher surface densities, in the range from $4.5 \cdot 10^{-4}$ till 10^{-3}, the spread of viscosities useful for attaining the 2:1 resonance shrinks to the interval from $4 \cdot 10^{-6}$ till 10^{-5}.

First, we investigate how the planets locked in the 2:1 resonance evolve in time in discs which differ among themselves only by the value of the viscosity, while the surface density is kept fixed. For this purpose we choose $\Sigma = 3 \cdot 10^{-4}$ because, as it is shown in Fig. 1, this value of the surface density gives us the biggest range of viscosities for which the resonance under consideration is possible. From our analysis it turns out that the semi-major axis ratios oscillate always around the position of the resonance and we can identify two characteristic behaviours of this oscillation. The first kind of behaviour appears if the viscosity is $3 \cdot 10^{-5}$ or lower. In that case the semi-major axis ratios oscillate with a large amplitude, the same for all discs. The second kind of behaviour occurs if the viscosity is higher than $3 \cdot 10^{-5}$ then the amplitude of the oscillations decreases together with increasing viscosity. Examples of these two behaviours are displayed in Fig. 4 (left panel) for two values of the kinematic viscosity, namely $5 \cdot 10^{-5}$ (black) and $3 \cdot 10^{-5}$ (grey). The amplitude of the oscillations is a straightforward consequence of the excitation of the Super-Earth eccentricity, shown in Fig. 4 (right panel). Let us also notice that after the capture in the mean motion commensurability the resonant interactions drive the eccentricities of the Super-Earth until their action is balanced by the circularization due to disc tides. For all discs with viscosities $3 \cdot 10^{-5}$ or lower we have observed that the eccentricities of the Super-Earth increase until they attain an equilibrium value of about 0.62. An example is given in Fig. 4 (right panel, grey line). For discs with very high viscosities there is still a lot of material in the vicinity of the Super-Earth, so the circularization forces act more efficiently and the final eccentricity (black curve in the right panel of Fig. 4) grows to a value lower than 0.62. Thus, there is a correlation between the final eccentricity and the surface density of the disc around the position of the Super-Earth. In the case of higher surface density the eccentricity is lower.

Next, we perform a similar investigation but this time we fix the value of the viscosity in the disc and check how the evolution of planets locked in the 2:1 resonance depends on the initial surface density of the disc (or equivalently on disc mass). The value of viscosity is taken to be $\nu = 10^{-5}$, which is a typical value for protoplanetary discs. In Fig. 5 we show the evolution of the semi-major axis ratios and the eccentricities of the Super-Earth for discs with this typical viscosity and two values of the surface density, namely $\Sigma = 10^{-4}$ (grey colour) and $\Sigma = 6 \cdot 10^{-4}$ (black colour). The value of the oscillation amplitude of the semi-major axis is again the consequence of the eccentricity evolution. The eccentricity

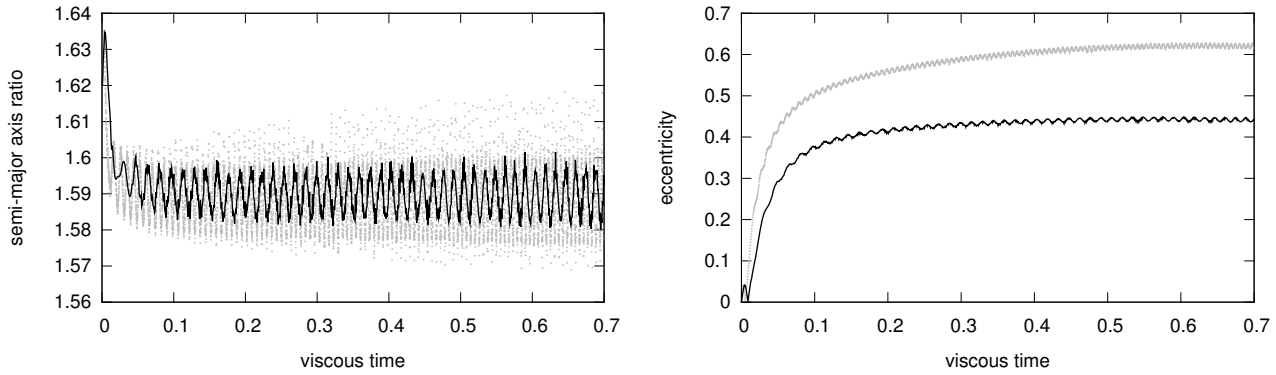

Figure 4. The evolution of the semi-major axis ratios (left panel), the Super-Earth eccentricities (right panel) due to the disc-planet interaction for two discs with the same surface density equal to $3 \cdot 10^{-4}$ and two values of the kinematic viscosity, namely $5 \cdot 10^{-5}$ (black) and $3 \cdot 10^{-5}$ (grey).

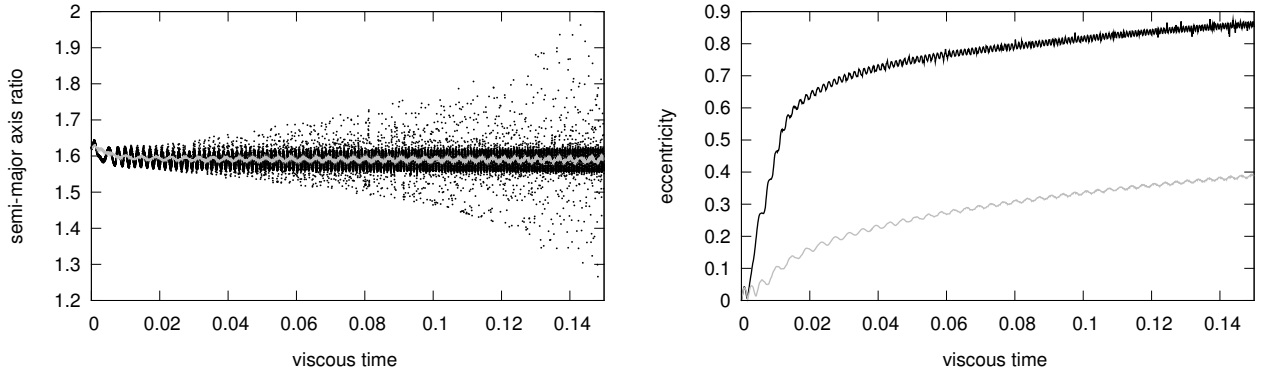

Figure 5. The evolution of the semi-major axis ratios (left panel), the Super-Earth eccentricities (right panel) due to the disc-planet interaction for two discs with the same viscosity equal to 10^{-5} and two values of the surface density, namely $6 \cdot 10^{-4}$ (black) and 10^{-4} (grey).

of the Super-Earth in the 2:1 resonance is bigger if the initial differential migration of the planets is faster which is in agreement with the Eq. (16) of Crida et al. (2008). It can be seen from Fig. 5 that both presented there eccentricities do not reach an equilibrium value. For the disc with higher surface density ($\Sigma = 6 \cdot 10^{-4}$) and viscosity $\nu = 10^{-5}$ it occurs, because the Super-Earth arrives at the inner edge of the disc before the eccentricity attains an equilibrium value. Instead, for the disc with lower surface density ($\Sigma = 10^{-4}$) and the same viscosity there is not enough material around the position of the Super-Earth in order to balance the resonant interactions. This is why the eccentricity continues to grow till the end of the run.

In all simulations in which the 2:1 resonance has been observed the angles between the apsidal lines and the resonant angles librate around zero. In Fig. 6 we plot the evolution of the angle between the apsidal lines (black colour) and the resonant angle, defined as $2\lambda_J - \lambda_s - \omega_s$ (grey colour) for $\Sigma = 10^{-4}$ and $\nu = 10^{-5}$. Here, λ_J and λ_s are the mean longitudes of the Jupiter and the Super-Earth respectively. The longitude of the pericentre of the Super-Earth is denoted by ω_s.

Our calculations have been able to determine also the lower limit of the viscosity necessary for the occurrence of the 2:1 resonance. We have noticed that below $\nu = 4 \cdot 10^{-6}$

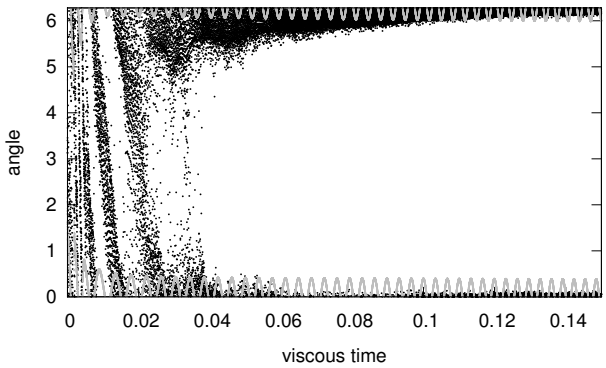

Figure 6. The evolution of the angles between the apsidal lines (black colour) and the resonant angle (grey colour) for the disc with the kinematic viscosity 10^{-5} and the surface density equals to 10^{-4}.

there is no possibility of attaining the commensurability because the differential migration becomes divergent.

4.2 Other configurations

In the previous Subsection we have singled out within the parameter space of typical physical properties of protoplan-

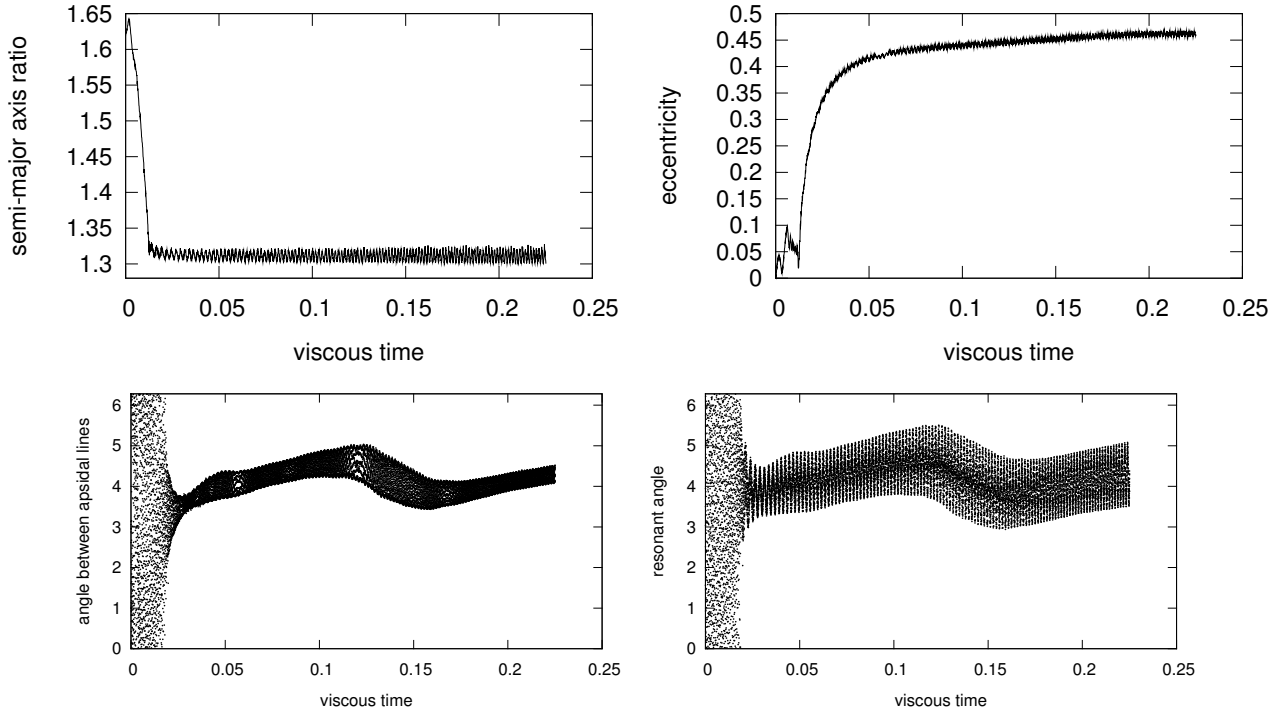

Figure 7. The evolution of the semi-major axis ratios (upper left panel), the Super-Earth eccentricities (upper right panel), the angle between the apsidal lines (bottom left panel) and the resonant angle (bottom right panel) due to the disc-planet interaction for a discs with the surface density: $6 \cdot 10^{-4}$ and the kinematic viscosity equal to $2 \cdot 10^{-5}$.

etary discs the region which is favourable for the achievement of the 2:1 resonance. We have also characterized the final configurations of the planets in this commensurability. However, the planet evolution in gaseous discs does not always end up in the 2:1 commensurability. In the following we would like to describe which are the alternatives to this behaviour and to determine the disc properties that lead to these different possibilities.

Let us start from the region in which the planets pass through the 2:1 resonance and approach the 3:2 commensurability. This is the small hatched region of Fig. 1 in which the surface densities vary between $4.5 \cdot 10^{-4}$ and $6 \cdot 10^{-4}$ in dimensionless units and the viscosities take their values in the narrow range $2-3 \cdot 10^{-5}$. For $\Sigma = 6 \cdot 10^{-4}$ and $\nu = 2 \cdot 10^{-5}$ the planets enter the 3:2 commensurability. The semi-major axis ratio oscillates around the value 1.32 (Fig. 7). The eccentricity of the Super-Earth reaches a value of 0.45 which is lower than what we get for the 2:1 commensurabilities. This result is in good agreement with that previously presented in Podlewska & Szuszkiewicz (2008) for the 3:2 resonance. The angle $\Delta\omega$ between the apsidal lines and the resonant angle librate around the value of 230 degrees (4 radians). Usually one observes that the equilibrium value of $\Delta\omega$ is either 0 or 180 degrees. However, it has been shown in Beauge et al. (2003) that $\Delta\omega$ is described by a function of the masses and the eccentricities of the two planets and that, for high eccentricities, it can librate around the values that are different from 0 or 180 degrees (e.g. Kley et al. (2004)). In a disc with the same surface density ($\Sigma = 6 \cdot 10^{-4}$) but with higher viscosity ($\nu = 3 \cdot 10^{-5}$), the 3:2 resonant trapping is also present, but it lasts only for roughly 470 orbits and after that the planets scatter. At the moment in which the planet scattering takes place, the eccentricity of the Super-Earth equals 0.38. The 3:2 commensurability has been achieved also in a disc with the surface density $\Sigma = 4.5 \cdot 10^{-4}$ and the viscosity $\nu = 3 \cdot 10^{-5}$. In this case, the eccentricity of the Super-Earth is equal to 0.3. The system does not abandon the 3:2 commensurability till the end of our simulations. For the same surface density $\Sigma = 4.5 \cdot 10^{-4}$ and lower viscosity ($\nu = 2 \cdot 10^{-5}$) we have again scattering in the system, but this time it occurs after staying for 400 orbits in the 3:2 resonance.

Below the threshold of the viscosity necessary for the 2:1 resonant trapping, which occurs at $4 \cdot 10^{-6}$, the migration is divergent, see the light grey part in Fig. 1. This region of parameters does not contain resonances, so we will not discuss it any further.

More interesting is the white region of high viscosities of Fig. 1. In this part of the diagram we observe unstable behaviours leading to major changes in the planet configurations. One of the examples of those instabilities is shown in Fig. 8. It is the case of a disc with surface density equal to $4.5 \cdot 10^{-4}$ and viscosity $5 \cdot 10^{-5}$. The gas giant evolving in the disc captures the Super-Earth in the 5:3 mean-motion resonance, as it is indicated by the fact that the relevant resonant angle is librating around a constant value (see lower right panel of Fig. 8). At a certain time after the instant 0.1 in viscous time units the low-mass planet starts to go around its host star on a clearly chaotic orbit. Further evolution leads to the orbit crossing and the gas giant becomes the internal planet in the system. Moreover, the final configuration after the orbit crossing is close to the 1:2 resonance.

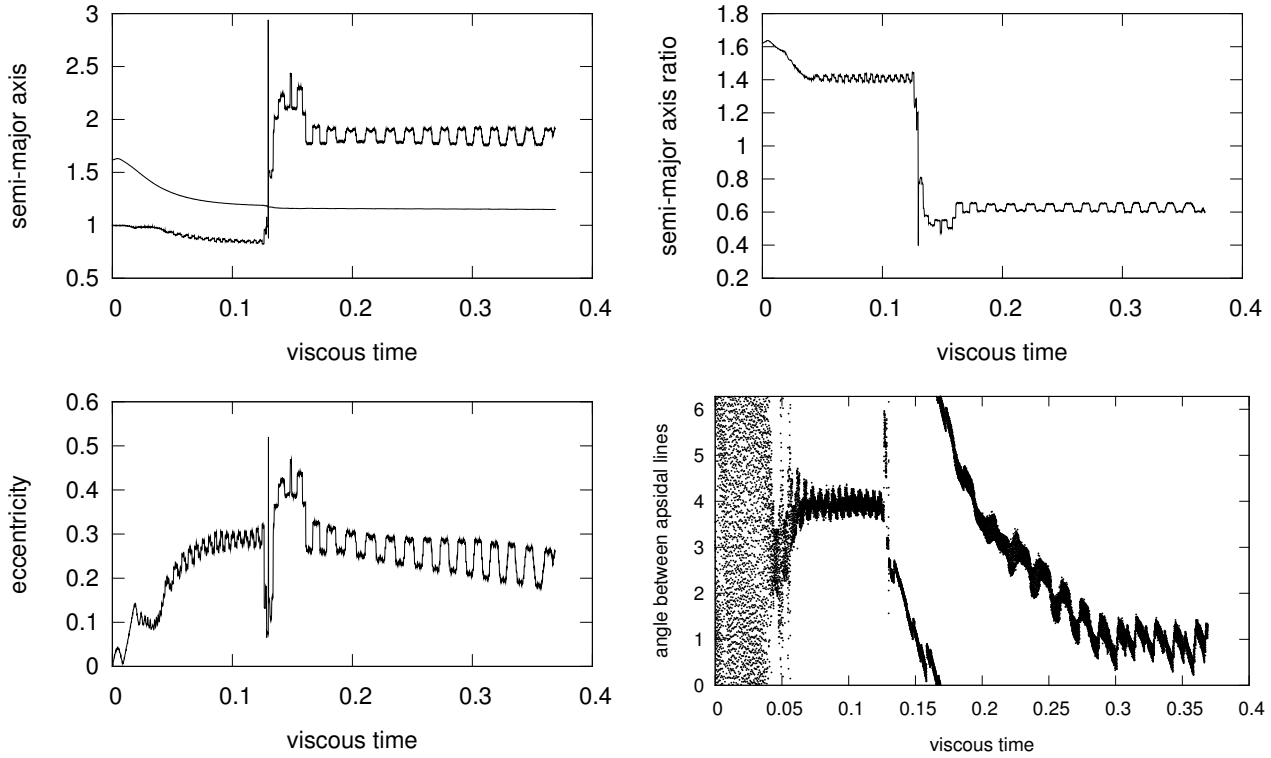

Figure 8. An example of unstable second order commensurability 5:3, which ends up with orbit crossing and evolves into a configuration close to the 1:2 resonance. The surface density is equal to $4.5 \cdot 10^{-4}$ and the viscosity has the value of $5 \cdot 10^{-5}$. The upper left panel shows the semi-major axis beheviour for both planets. The upper right panel illustrates the changes of the semi-major axis ratio in time. The lower left panel displays the evolution of the eccentricity of the Super-Earth orbit. Finally, the lower right panel presents the angle between the apsidal lines.

5 THEORETICAL ASPECTS OF THE RESONANCE SURVEY

In Fig. 1 we have shown the behaviour of the planets in the surface density-viscosity plane obtained from hydrodynamical simulations. It might be useful to compare our numerical results with those obtained from the analytical expressions for the migration speed provided in the literature. First, we assume that the Jupiter migrates according to the type II migration (Lin & Papaloizou (1993); Crida & Morbidelli (2007)) and its migration time can be estimated by

$$\tau_{II} = \frac{(GM)^{1/2} m_J r_J^{1/2}}{2\Gamma_{II}} \tag{4}$$

where r_J denotes the radial position of the gas giant, m_J is the mass of the gas giant, and Γ_{II} is the torque acting on the Jupiter. The torque is given by the following expression (Crida & Morbidelli 2007)

$$\Gamma_{II} = 2\pi r^+ \Sigma_{LP}(r^+) v_r(r^+) \sqrt{GMr^+} \tag{5}$$

where

$$\Sigma_{LP}(r,t) = \Sigma_0 T^{-5/4} \Big(\frac{\sqrt{r} - \sqrt{R_{inf}}}{\sqrt{r}} \Big) \exp(-a(GMr)^2/T)$$

is a surface density profile taken from Lynden-Bell & Pringle (1974). Here, $T = 12a\nu t + 1$ is a function of kinematic viscosity ν and time t, R_{inf} is the inner edge of the disc, Σ_0 and a are constants defining the initial shape of the surface density distribution. The radial velocity v_r as well as all other quantities in the expression for the torque acting on the planet is evaluated at the external edge of the gap opened by the gas giant, namely at $r^+ = r_J + 2R_H$ where R_H is the radius of the Hill sphere. Having specified the migration time for the gas giant we turn our attention to the Super-Earth. The evolution of the Super-Earth proceeds according to the type I migration as described in Tanaka et al. (2002)

$$\tau_I = (2.7 + 1.1p)^{-1} \frac{M}{m_s} \frac{M}{\Sigma_s {r_s}^2} h^2 {\Omega_s}^{-1} \tag{6}$$

where p denotes the surface density slope of the disc (see Eq. (1)), m_s is the mass of the Super-Earth and Ω_s is the angular velocity at the Super-Earth location r_s. Thus, we can easily predict when the differential migration will be convergent, which is essential for the occurrence of the mean-motion resonance. From the Eqs. (5) and (6) the criterion for the convergent migration reads

$$\nu \quad > \quad \frac{(1.364 + 0.541p)}{3\pi} \times \frac{\left(\frac{r_J}{r^+}\right)^{1/2} \left(\frac{m_s}{M}\right) \left(\frac{m_J}{M}\right) \left(1 - \left(\frac{R_{inf}}{r^+}\right)^{1/2}\right)}{h^2 \left(1 - \frac{4a}{T}(GMr^+)^2 \left(1 - \left(\frac{R_{inf}}{r^+}\right)^{1/2}\right)\right)} \tag{7}$$

Moreover, we can combine the expected differential migration speed with the strength of the 2:1 and 3:2 commensurabilities given by Quillen (2006), Mustill & Wyatt (2011) in order to guess if the capture will take place or not.

The resonant capture for the first order resonances in the restricted three body problem occurs when

$$\frac{1}{\frac{1}{\tau_I}-\frac{1}{\tau_{II}}} \geqslant \frac{3\pi}{\dot{\eta}_{crit}\Omega} \tag{8}$$

where $\dot{\eta}_{crit}$ is the critical mean motion drift rate and Ω is the angular velocity of the Jupiter. In the case of internal 2:1 resonance $\dot{\eta}_{crit} = 22.7(m_J/M)^{4/3}$ and for the 3:2 commensurability $\dot{\eta}_{crit} = 126.4(m_J/M)^{4/3}$ (Quillen 2006). Finally, we make an attempt to draw the theoretical analog of our Fig. 1. The results are shown in Fig. 9 (left panel). In this figure we have used the same grey scale and patterns as in Fig. 1 in order to facilitate the comparison.

The overall theoretical picture is similar to the one obtained in our numerical simulations. However, the details do not match exactly. The convergent migration takes place for viscosities higher than $1.2\cdot10^{-6}$. This gives the region of the divergent migration smaller than in Fig. 1. The region of the 2:1 resonance occurrence in both numerical and theoretical approaches occupies almost the same place in the space of the disc parameters. The only significant differences are present for relatively low surface densities and high viscosities. The hatched region with high viscosities (see Fig. 9, left panel) for which there are the conditions for the 3:2 commensurability, is much more extended than the analogous region that results from our numerical simulations. In the white region we expect the 4:3 commensurability. However, we would like to stress here that the picture discussed above has been obtained under the assumptions that the planets evolve according to classical type I and type II migrations.

In a more realistic situation, when the gap opened by the gas giant is not deep and clean the torque acting on the planet needs to be modified (Crida & Morbidelli (2007)). Therefore, in a more refined approximation, we have changed the assumption about gas giant migration. Namely, instead of applying Eq.(10) of Crida & Morbidelli (2007) as we did in order to obtain the diagram displayed in Fig. 9 (left panel) we use Eq.(15) of that work, so now the torque reads

$$\begin{aligned}\Gamma \quad &= 2\pi r^+\Sigma_{LP}(r^+)v_r(r^+)\sqrt{GMr^+}\times \\ &\left[1-f(P)-\frac{10R_H}{\pi r^+}\frac{\Omega_J {r_J}^2}{\sqrt{GMr^+}}\frac{v_r(r_J)}{v_r(r^+)}f(P)\frac{d\log\Sigma/B}{d\log r}\right]\end{aligned} \tag{9}$$

where Σ is the density inside the gap, B is the second Oort constant. The function

$$f(P)=\begin{cases}(P-0.541)/4 & \text{if } P<2.4646\\ \\ 1-\exp(-P^{0.75}/3) & \text{if } P\geqslant 2.4646\end{cases}$$

describes the gap depth expressed as a ratio of the gap surface density to the unperturbed density at r^+ and P is defined by

$$P=\frac{3H}{4R_H}+\frac{50}{(m_J/M)R}\lesssim 1$$

where R is the Reynolds number. In this way we are able to take into account the torque exerted on the outer disc by the gas in the gap and the corotation torque. The resulting picture can be viewed in Fig. 9 (right panel). As it is possible to see in this figure the hatched area has shrunk towards higher values of the surface density, which is in better agreement with the numerical findings. The region of the divergent migration for low viscosities remains unchanged. This is because, for low viscosities, the torque expressed by Eq. (5) is very similar to that of Eq. (9), so the line dividing the regions of the divergent and convergent migrations can be obtained from Eq. (7) also in this case. Moreover, the region of the divergent migration has appeared for high viscosities as expected. Whenever the migration is convergent, the planets will be captured either in the 2:1 or 3:2 resonances. The line between the regions of the occurrence of these commensurabilities can be found using the criterion Eq. (8) in which τ_{II} is expressed by Eq. (4), but Γ_{II} is replaced by the torque given by Eq. (9). The stability of the resonances requires further studies. Other methods must be used in order to determine the final outcome of the migration of the resonant pair of planets. The numerical approach demonstrates to be very useful to tackle such problems and enables us to identify those regions in the parameter space in which the commensurabilities are not only form, but also are maintained at least for the time accessible to full hydrodynamic calculations. In Fig. 1 those regions has been indicated by the medium grey colour and the hatched pattern. The rest of the parameter space, where the migration of planet is convergent has been left in white. The whole variety of behaviours has been observed in this white region including transient second order resonances and the orbit crossing, which indicates that not all resonant captures shown in Fig. 9 are stable.

As already explained, in order to draw Fig. 9 we have used the assumption that the Super-Earth migrates according to Tanaka et al. (2002), but recently it has been shown by Paardekooper & Mellema (2006), Baruteau & Masset (2008), Kley & Crida (2008), Paardekooper et al. (2010, 2011) that in non-locally isothermal discs the rate and even the direction of the type I migration can be strongly changed. Therefore, we discuss briefly how our results would be affected by considering non-locally isothermal discs. If the Super-Earth migrates inward slower than in our simulations we would observe a faster differential migration and in consequence the regions of occurrence of the 2:1 resonance in our surface density-viscosity plane would be shifted downward. In the situation, when the Super-Earth migrates inward faster than in our calculations, it would be more difficult to obtain the convergent migration. Thus, the regions of occurrence of the 2:1 resonance would be shifted upward. However, we expect that the global picture should be similar. In the case of the Super-Earth migrating outwards, the most likely effect would be the scattering of the low-mass planet.

We have also checked the influence of the surface density profile on our final results. In our calculations we have used the initial density profile with power-law index $p = 0$, while the observations suggest $0.5 < p < 1.5$ (Pietu et al. 2007). In doing that, we have run simulations with $p = 1$ taking $\Sigma = 6\cdot10^{-4}$ and viscosities $\nu = 10^{-6}, 10^{-5}, 2\cdot10^{-5}, 3\cdot10^{-5}$ and $8\cdot10^{-5}$. It has been found that the differential migration is slower than for $p = 0$, so that the global picture is qualitatively the same but the regions of the characteristic behaviours in Fig. 1 are moved upward. For example the case with $\Sigma = 6\cdot10^{-4}$ and $\nu = 2\cdot10^{-5}$ gives the 3:2 resonance for the disc with $p = 0$. In the same disc with power-law index $p = 1$ we have obtained the 2:1 commensurability.

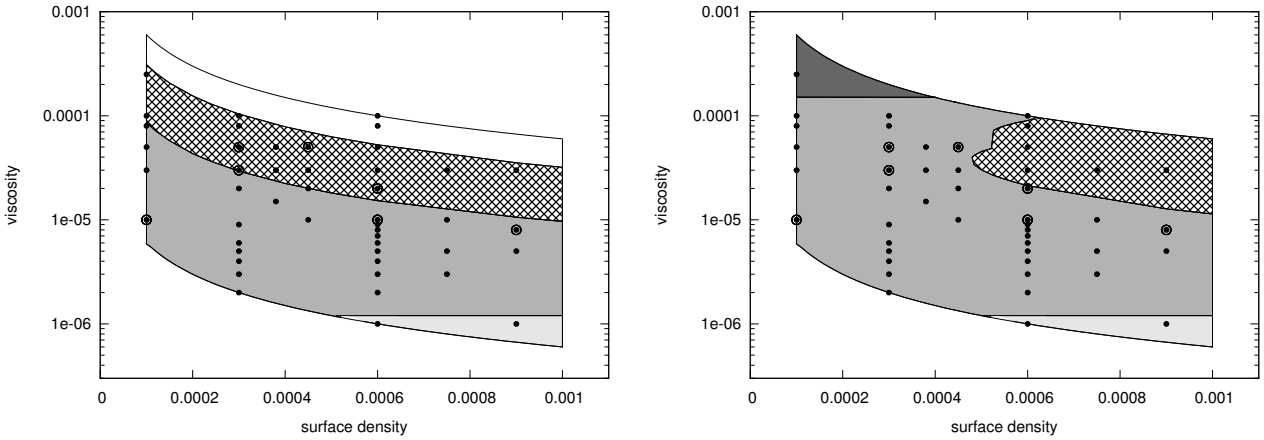

Figure 9. The parameter space of the properties of the protoplanetary discs: surface density - viscosity plane obtained under the assumptions that the planets evolve according to the classical type I and type II migration respectively (left panel) and that the evolution of the Super-Earth is the type I migration and that of the Jupiter is modified by the gas possibly present in the gap (Crida & Morbidelli 2007) (right panel).

Moreover, as we have mentioned in Section 2, we do not exclude any material from the Hill sphere. To justify our approach, we have performed numerical simulations in order to investigate the influence of the material close to the planet on the gas giant migration rate. We have observed that excluding the material from the Hill sphere results in the slowing down of the migration of the Jupiter, which has been already shown by Crida et al. (2009). Thus, the differential migration is also slowed down and the global picture would be the same as taking higher p. That means that the region of the resonant behavior will be shifted toward higher viscosities in our parameter space.

6 OBSERVATIONAL ASPECTS OF THE RESONANCE SURVEY

In our calculations we have started the investigations by choosing the masses of the planets and setting the main properties of the protoplanetary disc in which they are embedded, namely its surface density distribution, aspect ratio and viscosity. Ideally, one would like to use observed quantities in order to fix the initial conditions for such calculations. However, regardless of the fact that circumstellar discs are the natural outcome of the star-formation process, their structure is still not known in sufficient details in order to set such conditions using direct measurements.

The most powerful technique which could be able to change this situation and provide the most common properties of protoplanetary discs, is that of high resolution imaging. Recently, Isella et al. (2010) have presented the CARMA (Combined Array for Research in Millimeter-wave Astronomy) observations of the thermal dust emission from the discs around RY Tau and DG Tau with the best resolution achieved to date at wavelengths of 1.3 mm and 2.8 mm, namely 0.15" (which gives 20 AU at the distance of the Taurus cloud). On the basis of their high angular resolution observations, Isella et al. (2010) have determined the disc properties of these objects. Unfortunately, at radii smaller than 15 AU, which are the most relevant for our studies discussed here, the surface density is model dependent and can vary by almost an order of magnitude. In our work, as mentioned in Section 2, we simply assume the classical power law parameterization of Eq. 1 with $p = 0$. A better assumption for the surface density distribution will be possible only with the future advances in observational techniques. Taking the values of the surface density derived by Isella et al. (2010) we have placed DG Tau and RY Tau in the diagram of Fig. 1. The result is displayed in Fig. 10 which shows the same regions as Fig. 1. DG Tau is located in that region of the parameter space in which a 3:2 resonance might be achieved but it is not preserved. In the case in which planets would be present in DG Tau, the most likely scenario would be the temporary Super-Earth capture into 3:2 commensurability by the Jupiter-like planet and then scattering. This case has been described shortly in Section 4.2. Also for the RY Tau we do not expect the 2:1 commensurability. If in the inner disc of RY Tau there would be a pair of planets similar to that considered in our paper, then the Jupiter-like planet would migrate outwards and the Super-Earth inwards. The divergent migration would not induce any commensurability.

We have also collected from the literature the observed properties of the circumstellar discs around other young stars. In Fig. 10 we have marked the location of several observed systems. Rox 44, UX Tau A and LkCa 15 have been observed and modelled by Espaillat et al. (2010). The data has been taken from their Table 3. The physical properties of Rox 44 and UX Tau A indicate the possibility of the occurrence of the 2:1 commensurability. This is also the case of GM Aur studied by Hughes et al. (2009). Instead, the disc in LkCa 15 is located well below the region where the resonant structure can be expected. If planets were present in this disc, the gas giant would migrate slower than the Super Earth and, since the Jupiter is on the external orbit, it would not be able to catch the Super-Earth and form the mean-motion resonance. The open circles are the locations of ten other discs studied by Andrews et al. (2010), namely Elias 24, GSS 39, DoAr 25, WAOph 6, VSSG 1, SR 4, SR 13, WSB 52, WL 18 and SR 24 S. They belong to the 1 Myr-old Ophiuchus star forming region. Two of those, namely DoAr 25 and SR 13, share almost the same properties and

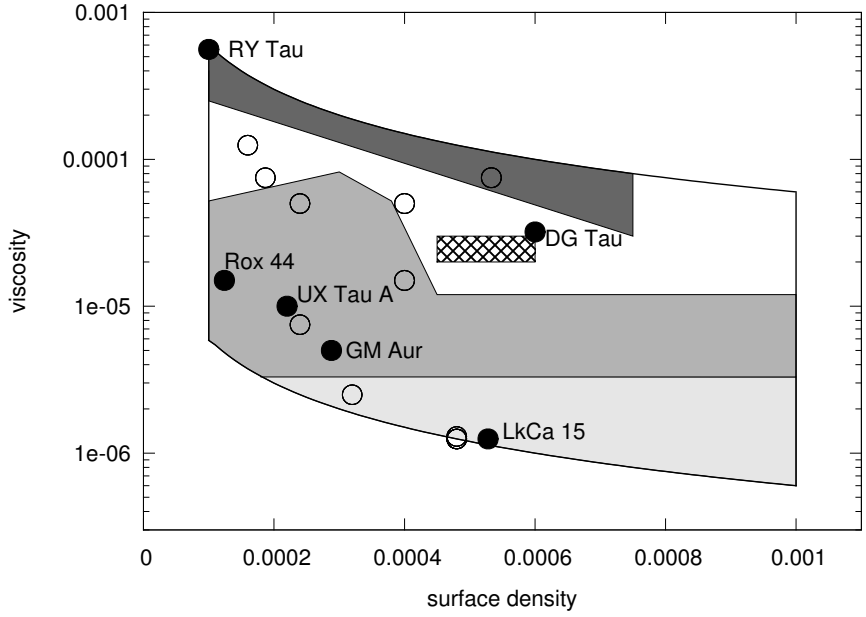

Figure 10. The surface density - viscosity plane with the positions of several interesting protoplanetary discs. See text for full description.

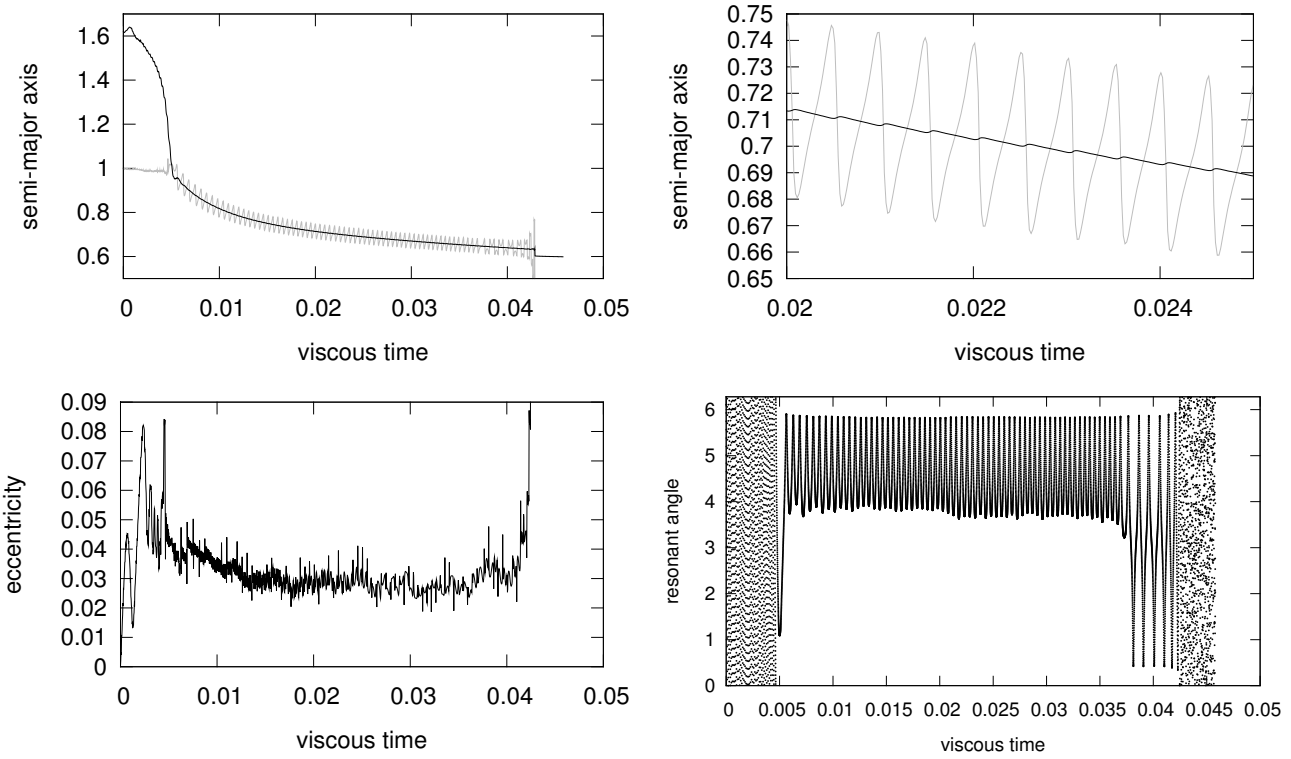

Figure 11. An example of the 1:1 commensurability, which ends with the ejection of the Super-Earth from the system. The two upper panels show the semi-major axis evolution for both planets. The upper right panel is a zoomed out version of the short time interval presented in the upper left panel. The lower left panel presents how the Super-Earth eccentricity changes in time and lower right panel illustrates the behaviour of the resonant angle.

are located very close to each other in our picture of the parameter space.

Of course, the predictions coming from the observations are still somewhat vague due to the huge uncertainties in the determination of the disc structure parameters. The purpose of this Section was however to stress the fact that such predictions are already possible and can be tested in the future with the advances of the observational techniques.

7 DISCUSSION AND CONCLUSIONS

In this paper we have constrained the properties of protoplanetary discs which favour the locking of a Super-Earth and a Jupiter-like planet orbiting around a Sun-like star in the 2:1 commensurability. The Super-Earth and the Jupiter are located on the internal and external orbits respectively. The results are illustrated in Figs. 1 and 10. In both figures the medium grey region is where we expect the 2:1 resonance to occur. In the low surface density regime (less or equal to $4 \cdot 10^{-4}$) the final outcome is relatively easy to determine. The migration of both planets is rather slow in this region. We expect the 2:1 resonance for viscosities not lower than $4 \cdot 10^{-6}$. Below this threshold the Jupiter migrates slower than the Super-Earth and no commensurability can be achieved. On the other side, in order to get the 2:1 resonance, the viscosity cannot be too high, because then the Jupiter will migrate outwards. This is the case in which the viscosity combined with the surface density through Eq. (2) gives accretion rates higher than 10^{-7} $M_{\odot}$/yr. In the high surface density regime (higher than $6 \cdot 10^{-4}$) the situation is more complicated and the 2:1 resonance is allowed only in a narrow strip where the viscosity is varying in the range from $4 \cdot 10^{-6}$ till 10^{-5}. In this regime the equilibrium gap profile is not empty. This is particularly true for relatively high viscosities. For that reason, putting the gas giant in the disc results in its very rapid migration. To avoid the artefact caused by the process of gap opening, we kept the Jupiter-like planet fixed, not allowing for its migration till the gap has reached the quasi-stationary state and stops changing significantly. In this way we have obtained the 2:1 resonance for viscosities ranging from $4 \cdot 10^{-6}$ till 10^{-5}. The results coming from numerical simulations have been compared with the analytical predictions summarized in Fig. 9 and with the current observations, see Fig. 10.

The orbital migration of planets embedded in protoplanetary discs is a natural mechanism in which resonant configurations might occur. However, it is not the only way to form orbital commensurabilities. It has been suggested that the planet-planet scattering might be an efficient mechanism leading to the resonant capture of planets (Raymond et al. 2008). Our computational set up allows us to investigate also this scenario in the situation when the gaseous disc is still present in the system. We have employed a simple procedure to locate both planets in a disc with high surface density (higher than $6 \cdot 10^{-4}$) and let them migrate without waiting for the Jupiter to open a gap. Here we discuss in details one example of resonance obtained in this way. Our probe, which consists of a Jupiter-like planet and a Super-Earth, is located in a disc with surface density equal to $9 \cdot 10^{-4}$ and viscosity value taken to be $8 \cdot 10^{-6}$. As expected, the Jupiter migrates extremely fast (with type III migration, Masset & Papaloizou (2003)), traveling one third of the distance from its initial location to the star in just 100 orbits. Its orbit crosses the orbit of the slowly migrating Super-Earth and we witness a resonant capture into 1:1 mean motion resonance. This is shown in Fig. 11 (two upper panels). After the occurrence of the locking the Super-Earth stays very close to the Jupiter on the horseshoe orbit with an eccentricity of about 0.03 (Fig. 11, left lower panel). The resonant angle is shown in Fig. 11 (right lower panel). The 1:1 commensurability created in the way described above lasted for roughly 700 orbits and after that the Super-Earth has been ejected from the system.

Concluding, we have shown how the mean-motion resonances observed in the already formed planetary systems can help in getting additional insight into the conditions occurring in protoplanetary discs in the early phases of the planetary system evolution. In other words, we have made an attempt to constrain the resonant properties of the planetary systems which may occur in observed protoplanetary discs. Assuming that the resonances are due to early stages of the evolution, we can answer the question on what should be the disc properties in order to attain the 2:1 resonance.

ACKNOWLEDGMENTS

This work has been partially supported by MNiSW grant N203 026 32/3831 (2007-2010) and MNiSW PMN grant - ASTROSIM-PL "Computational Astrophysics. The formation and evolution of structures in the universe: from planets to galaxies" (2008-2010). We acknowledge support from the Isaac Newton Institute programme "Dynamics of Discs and Planets". Part of this research was performed during a stay at the Kavli Institute for Theoretical Physics, and was supported in part by the National Science Foundation under Grant No. PHY05-51164. The simulations reported here were performed using the HAL9000 cluster of the Faculty of Mathematics and Physics of the University of Szczecin. We thank the referee for valuable comments which helped us in improving the manuscript. We are grateful to John Papaloizou for enlightening discussions. We wish also to thank Adam Łacny for his helpful comments. Finally, we are indebted to Franco Ferrari for his continuous support in the development of our computational techniques and computer facilities.

REFERENCES

Agol, E., Steffen, J., Sari, R., & Clarkson, W. 2005, MNRAS, 359, 567
Andrews, S. M., Wilner,D. J., Hughes, A. M., Qi, C. and Dullemond, C.P., 2009, ApJ, 700, 1502
Andrews, S. M., Wilner,D. J., Hughes, A. M., Qi, C. and Dullemond, C.P., 2010, ApJ, 723, 1241
Baruteau, C., Masset, F., 2008, ApJ, 672, 1054
Beauge, C., Ferraz-Mello, S., Michtchenko, T. A., 2003, ApJ, 593, 1124
Crida, A., Morbidelli, A., 2007, MNRAS, 377, 1324
Crida, A., Baruteau, C., Kley, W., Masset, F., 2009, A& A, 502, 673
Crida, A., Sandor, Z., Kley, W., 2008, A&A, 483, 325
Espaillat, C., DAlessio, P., Hernandez, J., Nagel, E., Luhman, K. L., Watson, D. M., Calvet, N., Muzerolle, J., McClure, M., 2010, ApJ, 717, 441
Fogg, M. J., Nelson, R. P., 2007, A&A. 472, 1003
Hayashi, C., 1981, Prog. Theor. Phys. Suppl.,70, 35
Holman, M. J., & Murray, N. W. 2005, Science, 307, 1288
Huélamo, N.; Lacour, S., Tuthill, P., Ireland, M., Kraus, A., Chauvin, G., 2011, A&A, 528, L7
Hughes, A. M., Andrews S. M., Espaillat C., and 7 coauthors, 2009, ApJ, 698, 131

Isella, A., Carpenter, J. M., Sargent, A. I. 2010, ApJ, 714, 1746
Kley, W., Crida, A., 2008, A& A, 487, L9
Kley, W., Peitz, J., Bryden, G., 2004, A& A, 414, 735
Lin, D. N. C., Papaloizou, J. C. B., 1986, ApJ, 309, 846
Lin, D. N. C., Papaloizou, J. C. B., 1993, Protostars and planets III, 749
Lovis, C., Ségransan, D., Mayor, M., and 11 coauthors, 2011, A&A, 528, A112
Lynden-Bell, D., Pringle, J. E., 1974, MNRAS, 168, 603
Mandell, A. M., Sigurdsson, S., 2003, ApJ, 599, L111
Masset, F. S.; Papaloizou, J. C. B., 2003, ApJ, 588, 494
Mayor, M., Udry, S., Lovis, C., and 9 coauthors, 2009a, A&A, 493, 639
Mayor, M., Bonfils, X., Forveille, and 10 coauthors, 2009b, A&A, 507, 487
Mustill, A. J., Wyatt, M. C., 2011, MNRAS, 413, 554
Nelson R. P., Papaloizou J.C. B., Masset F., Kley W., 2000, MNRAS, 318, 18
Nelson R. P., Papaloizou J.C. B., 2002, MNRAS, 333, L26
Olofsson, J., Benisty, M., Augereau, J.-C. and 11 coauthors, 2011, A&A, 528, L6
Paardekooper, S.-J.; Mellema, G., 2006, A& A, 459, L17
Paardekooper, S.-J., Papaloizou, J. C. B., 2008, A&A, 485, 877
Paardekooper S.-J., Papaloizou J. C. B., 2009, A&A, 394, 2297
Paardekooper, S.-J., Baruteau, C., Crida, A., Kley, W., 2010, MNRAS, 409, 1950
Paardekooper, S.-J., Baruteau, C., Kley, W., 2011, MNRAS, 410, 293
Papaloizou, J. C. B., Szuszkiewicz, E., 2005, MNRAS, 363, 153
Papaloizou, J. C. B., Szuszkiewicz, E., 2010, in *Extrasolar Planets in Multi-Body Systems: Theory and Observations*, K. Goździewski, A. Niedzielski and J. Schneider (eds), EAS Publication Series, 42, 333
Pietu, V., Dutrey, A., Guilloteau, S., 2007, A& A, 467, 163
Podlewska, E., Szuszkiewicz, E., 2008, MNRAS, 386,1347
Podlewska, E., Szuszkiewicz, E., 2009, MNRAS, 397.1995
Quillen, A. C., 2006, MNRAS, 365, 1367
Raymond, S. N., Mandell, A. M., Sigurdsson, S., 2006, Science, 313, 1413
Raymond, S. N., Barnes R., Armitage P. J., Gorelick N., 2008, ApJ, 687, L107
Tanaka, H., Takeuchi, T., Ward, W. R., 2002, ApJ, 565, 1257
Ward, W. R., 1997, Icarus, 126, 261
Zhou, J. -L, Aarseth, S. J., Lin, D. N. C., Nagasawa, M., 2005, ApJL, 631, 85